Environmental Microbiology (2008) **10**(1), 110–124 doi:10.1111/j.1462-2920.2007.01437.x

Latitudinal trends of *Crenarchaeota* and *Bacteria* in the meso- and bathypelagic water masses of the Eastern North Atlantic

Marta M. Varela,[1] Hendrik M. van Aken,[2] Eva Sintes[1] and Gerhard J. Herndl[1]*

Departments of [1]Biological Oceanography and [2]Physical Oceanography, Royal Netherlands of Sea Research (NIOZ), 1790 AB Den Burg, the Netherlands.

Summary

The distribution and activity of the bulk picoplankton community and, using microautoradiography combined with catalysed reported deposition fluorescence *in situ* hybridization (MICRO-CARD-FISH), of the major prokaryotic groups (*Bacteria*, marine *Crenarchaeota* Group I and marine *Euryarchaeota* Group II) were determined in the water masses of the subtropical North Atlantic. The bacterial contribution to total picoplankton abundance was fairly constant, comprising ~50% of DAPI-stainable cells. Marine *Euryarchaeota* Group II accounted always for < 5% of DAPI-stainable cells. The percentage of total picoplankton identified as marine *Crenarchaeota* Group I was ~5% in subsurface waters (100 m depth) and between 10% and 20% in the oxygen minimum layer (250–500 m) and deep waters [North East Atlantic Deep Water (NEADW) and Lower Deep Water (LDW), 2750–4800 m depth]. Single-cell activity, determined via a quantitative MICRO-CARD-FISH approach and taking only substrate-positive cells into account, ranged from 0.05 to 0.5 amol D-aspartic acid (Asp) cell^{-1} day^{-1} and 0.1–2 amol L-Asp cell^{-1} day^{-1}, slightly decreasing with depth. In contrast, the D-Asp:L-Asp cell-specific uptake ratio increased with depth. By combining data reported previously using the same method as applied here and data reported here, we found a decreasing relative abundance of marine *Crenarchaeota* Group I throughout the meso- and bathypelagic water column from 65°N to 5°N in the eastern basin of the North Atlantic. Thus, the relative contribution of marine *Crenarchaeota* Group I to deep-water prokaryotic communities might be more variable than previous studies have suggested. This apparent variability in the contribution of marine *Crenarchaeota* Group I to total picoplankton abundance might be related to successions and ageing of deep-water masses in the large-scale meridional ocean circulation and possibly, the appearance of crenarchaeotal clusters other than the marine *Crenarchaeota* Group I in the (sub)tropical North Atlantic.

Received 24 June, 2007; accepted 11 August, 2007. *For correspondence. E-mail herndl@nioz.nl; Tel. (+31) 222 369 507; Fax (+31) 222 319 674.

Introduction

Over the past decade, the notion emerged that non-thermophilic planktonic *Archaea* constitute a major component of prokaryotic plankton in the ocean (DeLong, 1992; Fuhrman *et al*., 1992). Quantitative studies with fluorescence *in situ* hybridization (FISH) have revealed the high abundance of *Crenarchaeota* in meso- and bathypelagic waters of the subtropical Pacific Gyre (Karner *et al*., 2001), the northern North Atlantic (Herndl *et al*., 2005; Teira *et al*., 2006a) and Antarctic waters (Church *et al*., 2003). Also in the Arctic Ocean, a higher contribution of *Crenarchaeota* to total prokaryotic plankton was found in the mesopelagic waters than in surface waters (Kirchman *et al*., 2007). In contrast, euryarchaeotal abundance tends to be more stable throughout the water column (Karner *et al*., 2001; Church *et al*., 2003; Teira *et al*., 2006a,b).

All these studies indicate that *Archaea* and, particularly, *Crenarchaeota* might be ubiquitously distributed in the deep ocean. However, there are too few quantitative data on the distribution of *Crenarchaeota* in oceanic waters to allow firm conclusions on their global distribution and abundance in the meso- and bathypelagic oceanic realm.

Also, little is known on the metabolic capabilities of *Archaea* in pelagic marine environments. A few recent studies have shown that they are chemoautotrophic using inorganic carbon as a carbon source (Herndl *et al*., 2005; Ingalls *et al*., 2006; Wuchter *et al*., 2006). The only non-extremophilic crenarchaeal isolate, *Nitrosopumilus maritimus*, is oxidizing ammonia as an energy source (Könneke *et al*., 2005). However, this strain does not grow well at temperatures below 10°C (M. Könneke, pers. comm.) indicating that there might be differences in the physiological capabilities of this isolated crenarchaeote and the

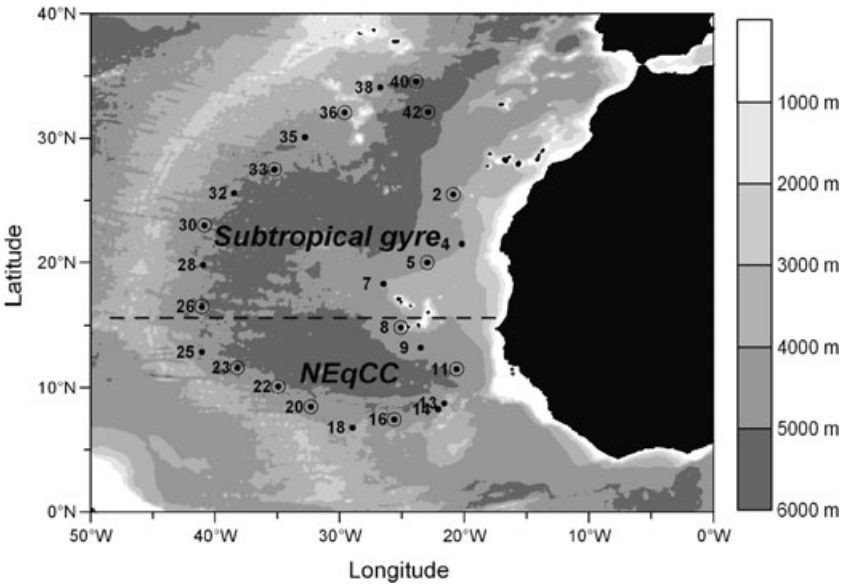

Fig. 1. Location of sampling stations in the (sub)tropical North Atlantic waters during the ARCHIMEDES-I cruise. Sampling stations are indicated by numbered dots. Broken line separates the stations of the subtropical gyre from those in the North Equatorial Counter Current (NEqCC). Encircled dots indicate stations where CARD-FISH samples were taken.

Crenarchaeota present in the oceanic deep waters. There are indications that pelagic *Crenarchaeota* are also heterotrophic or mixotrophs (Hallam *et al*., 2006) taking up amino acids (Ouverney and Fuhrman, 2000; Herndl *et al*., 2005; Teira *et al*., 2006a; Kirchman *et al*., 2007). While L-antiomeric amino acids present the vast majority of the total amino acid pool in the ocean and are efficiently taken up by the heterotrophic prokaryotic community, D-amino acids are considered refractory. Recently, it has been shown, however, that in meso- and bathypelagic waters of the North Atlantic *Crenarchaeota* are mainly responsible for the observed increase in the bulk D-:L-aspartic acid (Asp) uptake ratio with depth (Pérez *et al*., 2003; Teira *et al*., 2006a).

The goal of this study was to determine the distribution of *Archaea* and *Bacteria* in the main water masses of the (sub)tropical North Atlantic (from 35°N to 5°N) throughout the water column. In previous studies, the relative contribution of *Bacteria* and marine *Crenarchaeota* Group I and marine *Euryarchaeota* Group II was determined in the northern North Atlantic (from 65°N to 35°N) following the North East Atlantic Deep Water (NEADW) (Herndl *et al*., 2005; Teira *et al*., 2006a,b). The distribution pattern observed in these previous studies are combined with the results from the (sub)tropical North Atlantic to obtain a general distribution pattern of marine *Crenarchaeota* Group I along the main flow of the NEADW over the different oceanographic regions in the North Atlantic. By following the NEADW, a pronounced latitudinal gradient was found in the distribution of marine *Crenarchaeota* Group I declining in their relative contribution to total prokaryotic abundance from 65°N towards the equator throughout the water column. Also, the uptake of D- and L-Asp by the bulk prokaryotic community was determined and compared with the D- and L-Asp uptake on a single-cell level using the recently developed quantitative microautoradiography and catalysed reporter deposition fluorescence *in situ* hybridization (MICRO-CARD-FISH) approach (Sintes and Herndl, 2006).

Results

Meso- and bathypelagic water mass characteristics

Water masses along the subtropical North Atlantic transect (Fig. 1) were identified based on their temperature and salinity characteristics. The vertical distribution of temperature, salinity and oxygen along the cruise transect is shown in Fig. 2. Table 1 summarizes the basic physicochemical characteristics of the main water masses. At 4000 m depth, Lower Deep Water (LDW), characterized by low salinity (34.9) and temperature (2.3–2.6°C), consisted mainly of Antarctic Bottom Water coming from the south mixed with some NEADW. The NEADW, mainly formed by Iceland Scotland Overflow Water and Labrador Sea Water, is characterized by a seawater temperature between 2.8°C and 3.0°C and a higher oxygen content than LDW (Table 1). The core of NEADW was identifiable throughout the transect at around 2750 m depth. Two types of intermediate waters were found between 900 and 1100 m depth. In the subtropical gyre region, the intermediate waters were formed by the saline Mediterranean Sea Outflow Water (MSOW), while in the North Equatorial Counter Current (NEqCC), Antarctic Intermediate Water (AAIW) was present characterized by lower salinity and temperature than MSOW (Fig. 2 and Table 1). A local

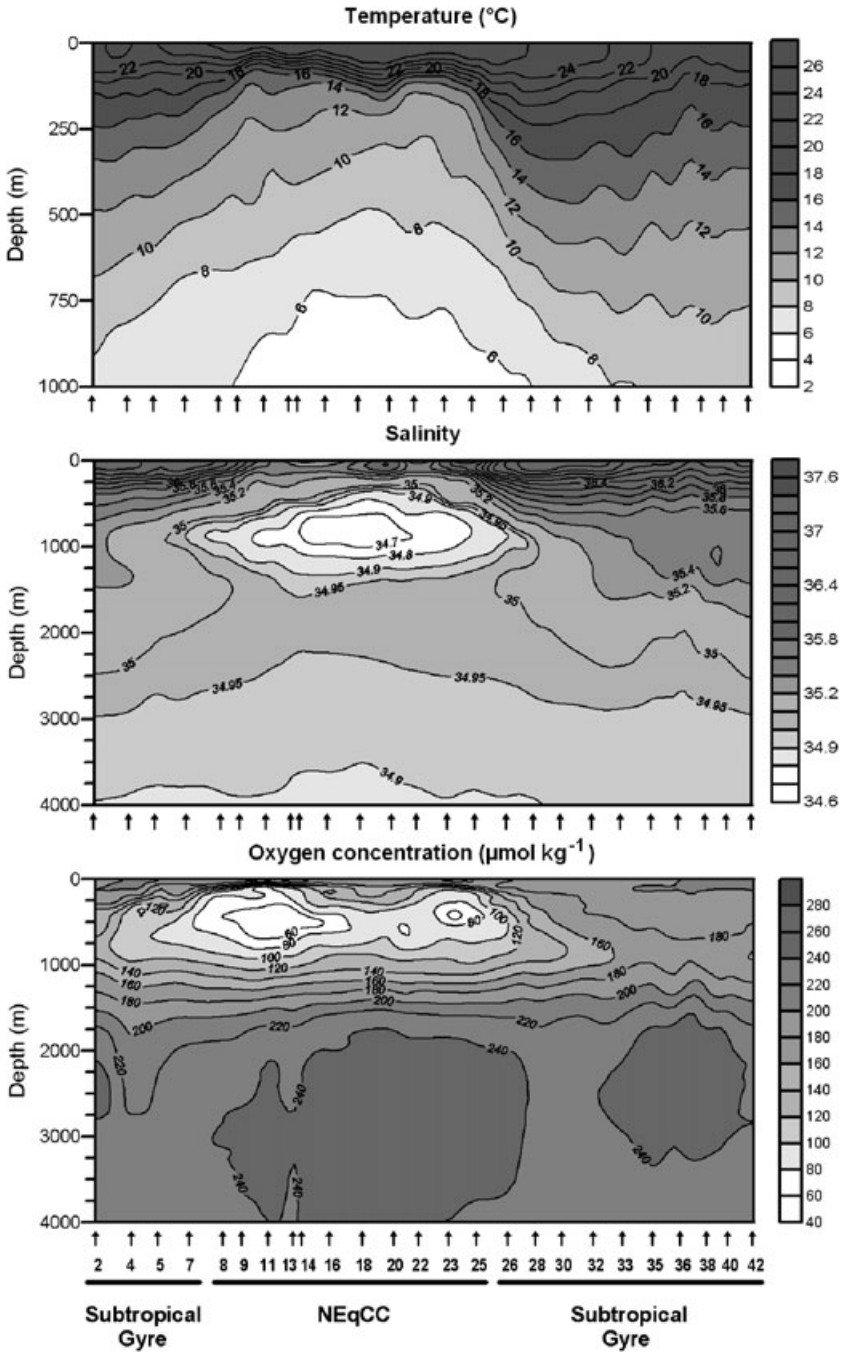

Fig. 2. Distribution of temperature, salinity and oxygen concentration in the (sub)tropical North Atlantic waters during ARCHIMEDES-I cruise. NEqCC, North Equatorial Counter Current.

oxygen minimum (< 100 µmol kg^{-1}) was found between 200 and 600 m in the north equatorial part of the transect [from stations (Sts.) 8–25] with oxygen concentrations < 60 µmol kg^{-1} at Sts. 11 and 23 (Fig. 2).

Picoplankton abundance and activity

Picoplankton abundance decreased exponentially with depth, ranging between 2.2 and 3.9×10^5 cells ml^{-1} at 100 m depth and from 0.1 to 0.8×10^5 cells ml^{-1} in the meso- and bathypelagic waters (Table 2). However, differences in picoplankton abundance between deep-water masses and regional trends were apparent. No significant differences, however, were found in the picoplankton abundance of the subsurface layer (100 m depth) between the subtropical gyre and the NEqCC (Mann–Whitney, $P > 0.05$, $n = 42$, Table 2). In the oxygen minimum layer, picoplankton abundance was higher in the NEqCC than in the corresponding water masses of the subtropical gyre (Mann–Whitney, $P < 0.01$, $n = 44$, Table 2). Also, in the

Table 1. Characteristics of the main water masses sampled during ARCHIMEDES-I based on CTD profiles at the individual stations.

Zone	Water mass	Depth (m)	Temperature (°C)	Salinity	Oxygen (μmol kg^{-1})
Subtropical gyre	Subsurface	100	17.7–24.1	36.4–37.5	138.9–221.5
	O_2-minimum	250–500	10.1–17.9	35.3–36.5	87.5–207.2
	MSOW	900–1000	7.6–9.2	35.1–35.6	121.2–197.7
	NEADW	2750	2.8–3.0	34.9	223.8–250.8
	LDW	3500–5000	2.4–2.6	34.9	223.7–242.5
NEqCC	Subsurface	100	14.2–18.5	35.5–36.4	79.6–132.7
	O_2-minimum	250–500	7.9–12.0	34.7–35.3	44.0–122.3
	AAIW	900	5.1–6.5	34.6–34.7	102.4–129.5
	NEADW	2750	2.8–3.0	34.9	234.3–247.1
	LDW	3750–4000	2.3–2.4	34.9	227.7–246.8

Ranges are given for each water mass where samples were collected.
MSOW, Mediterranean Sea Outflow Water; NEADW, North East Atlantic Deep Water; LDW, Lower Deep Water; AAIW, Antarctic Intermediate Water; NEqCC; North Equatorial Counter Current.

AAIW and deep waters (NEADW and LDW) of the NEqCC, picoplankton abundance was higher than in the MSOW and the deep-water masses (NEADW and LDW) of the subtropical gyre (Mann–Whitney, $P < 0.001$, $n = 22$, $P < 0.001$, $n = 43$, respectively, Table 2).

Leucine incorporation, as a measure of picoplankton activity, decreased with depth by two orders of magnitude (Table 2). Picoplankton activity in the subsurface waters was significantly higher in the subtropical gyre than in the NEqCC (Mann–Whitney, $P < 0.01$, $n = 21$). However, in the intermediate waters, picoplankton activity was higher in the AAIW than in the MSOW (Mann–Whitney, $P < 0.01$, $n = 22$), as was picoplankton abundance. While picoplankton activity was about twice as high in the NEADW of the NEqCC as in the subtropical gyre, picoplankton activity of the LDW was similar in both regions (Table 2).

Mean bulk L-Asp uptake rates decreased from 4.3 pmol l^{-1} h^{-1} at 100 m depth to 0.01 pmol l^{-1} h^{-1} in the LDW, while D-Asp decreased from 0.3 pmol l^{-1} h^{-1} at 100 m depth to 0.005 pmol l^{-1} h^{-1} in the NEADW (Table 2). The D-:L-Asp uptake ratio of the bulk prokaryotic community increased with depth in both the subtropical gyre and the NEqCC (Table 2). The highest D-:L-Asp uptake ratios (> 1) were measured in the LDW of the NEqCC at Sts. 18 and 23. No significant differences were found in the D-:L-Asp uptake ratio between the subtropical gyre and the NEqCC for any of the water masses [Mann–Whitney, $P > 0.05$, $n = 9$ for the subsurface, $n = 18$ for the oxygen minimum, $n = 8$ for the intermediate waters (MSOW and AAIW), $n = 12$ for the NEADW and $n = 9$ for the LDW].

Prokaryotic community composition

The abundance of *Bacteria*, marine *Crenarchaeota* Group I and marine *Euryarchaeota* Group II were determined by CARD-FISH at 14 stations regularly distributed along the transect (Fig. 1). For each sample, counts obtained with each of the specific probes were related to the abundance of DAPI-stainable cells referred to as picoplankton abundance. The number of DAPI-stained cells before and after CARD-FISH processing was not significantly different (*t*-test, $P > 0.05$, $n = 84$), indicating that cell losses during CARD-FISH processing were negligible. Picoplankton abundance determined by flow cytometry and picoplankton abundance determined by DAPI staining resulted in essentially the same abundance (slope = 0.99, $r^2 = 0.89$, $n = 71$, data not shown).

Table 2. Picoplankton abundance (PA) expressed in N × 10^5 cell ml^{-1}, leucine incorporation rates (Leu) and enantiomeric aspartic acid (Asp) uptake rates in pmol l^{-1} h^{-1} and the D-:L-Asp uptake ratio.

Zone	Water mass	PA N × 10^5 ml^{-1}	Leu pmol l^{-1} h^{-1}	D-Asp pmol l^{-1} h^{-1}	L-Asp pmol l^{-1} h^{-1}	D-:L-Asp
Subtropical gyre	Subsurface	3.24 ± 0.15	4.62 ± 0.68	0.29 ± 0.08	4.28 ± 1.05	0.06 ± 0.01
	O_2-minimum	1.00 ± 0.07	0.40 ± 0.09	0.05 ± 0.01	0.55 ± 0.25	0.11 ± 0.01
	MSOW	0.44 ± 0.04	0.03 ± 0.05	0.007 ± 0.001	0.07 ± 0.02	0.12 ± 0.01
	NEADW	0.15 ± 0.01	0.009 ± 0.001	0.005 ± 0.001	0.03 ± 0.01	0.22 ± 0.06
	LDW	0.16 ± 0.01	0.01 ± 0.003	0.004 ± 0.002	0.01 ± 0.001	0.30 ± 0.17
NEqCC	Subsurface	2.80 ± 0.18	2.31 ± 0.52	0.18 ± 0.07	1.86 ± 0.41	0.09 ± 0.01
	O_2-minimum	1.37 ± 0.07	0.45 ± 0.15	0.03 ± 0.01	0.37 ± 0.08	0.09 ± 0.01
	AAIW	0.65 ± 0.03	0.06 ± 0.02	0.01 ± 0.003	0.08 ± 0.02	0.13 ± 0.02
	NEADW	0.23 ± 0.01	0.02 ± 0.09	0.005 ± 0.002	0.03 ± 0.008	0.18 ± 0.05
	LDW	0.20 ± 0.01	0.01 ± 0.002	0.009 ± 0.005	0.01 ± 0.003	0.65 ± 0.30

Mean values ± SE are given. Water mass abbreviations as in Table 1.

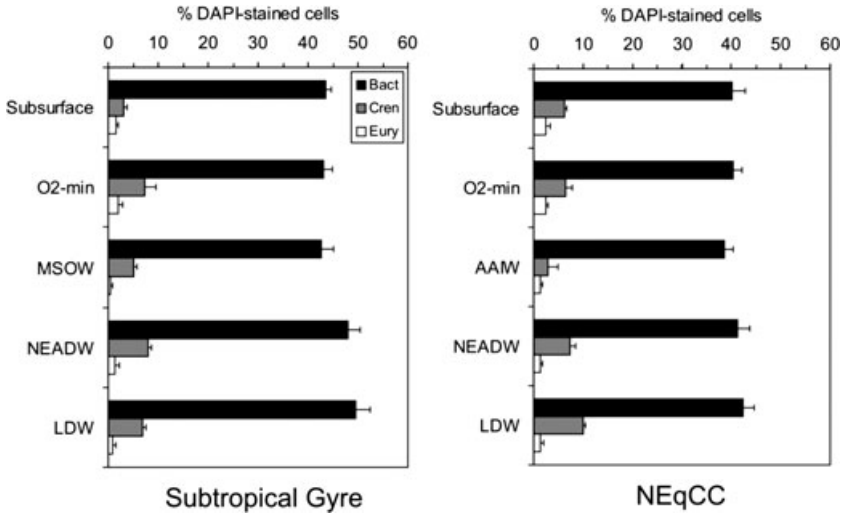

Fig. 3. Contribution of *Bacteria*, marine *Crenarchaeota* Group I and marine *Euryarchaeota* Group II to total picoplankton abundance in the different water masses of the (sub)tropical North Atlantic expressed as percentage of DAPI-stained cells. Bars represent means ± SE. NEqCC, North Equatorial Counter Current.

The mean contributions of *Bacteria*, marine *Crenarchaeota* Group I and *Euryarchaeota* Group II to total picoplankton abundance for the different water masses are given in Fig. 3. *Bacteria* contributed between 38% and 49% to total picoplankton abundance in the different water masses. Overall, the bacterial contribution to total picoplankton abundance was significantly higher (Mann–Whitney, $P < 0.01$, $n = 78$) in the subtropical gyre than in the NEqCC (Fig. 3). This was due to the higher contribution of *Bacteria* in the deep-water masses (NEADW and LDW) of the subtropical gyre (49% of DAPI-stained cells) than in the NEqCC (42% of DAPI-stained cells). However, in the water masses overlying the NEADW, no significant differences in the bacterial contribution to total picoplankton abundance were found between both regions (Fig. 3).

Marine *Crenarchaeota* Group I exhibited a more patchy distribution throughout the transect. The percentage of total picoplankton identified as marine *Crenarchaeota* Group I ranged between ~5% and > 15% in the subsurface waters and oxygen minimum layer or LDW respectively (Fig. 3). In general, marine *Crenarchaeota* Group I were more abundant in the NEqCC than in the subtropical gyre waters and the relative abundance was the highest in the oxygen minimum layer (up to 20% of DAPI-stained cells) and in the LDW (up to 15% of DAPI-stained cells). Marine *Euryarchaeota* Group II comprised always < 5% of DAPI-stainable cells (Fig. 3).

Distribution of D*-Asp and* L*-Asp uptake among* Bacteria*, marine* Crenarchaeota *Group I and marine* Euryarchaeota *Group II in the different water masses*

Both *Archaea* (marine *Crenarchaeota* Group I and *Euryarchaeota* Group II) and *Bacteria* were taking up D-Asp and L-Asp, although the distribution pattern of *Bacteria* and *Archaea* taking up D-Asp versus L-Asp revealed differences (Fig. 4). The percentage of *Bacteria* taking up L-Asp steadily decreased with depth from ~35% in the 100 m layer to about 10% in the LDW. The percentage of marine *Crenarchaeota* Group I taking up L-Asp did not follow this decreasing trend with depth but was the lowest in the oxygen minimum layer (Fig. 4). The percentage of *Bacteria* taking up D-Asp ranged from 13% in the surface layer to 5% in the LDW. The percentage of marine *Crenarchaeota* Group I taking up D-Asp, however, was the highest in the LDW (~8%) of the NEqCC and in the NEADW (~10%) of the subtropical gyre. The fraction of marine *Euryarchaea* Group II incorporating either D- or L-Asp was very low (< 5%) and Asp-positive cells were only found in subsurface and intermediate waters (Fig. 4).

No significant differences were found in the percentage of cells taking up D-Asp (Mann–Whitney, $P = 0.336$, $n = 58$) or L-Asp (Mann–Whitney, $P = 0.461$, $n = 57$) between the corresponding water masses of the subtropical gyre and the NEqCC (Fig. 4). Overall, the percentage of cells taking up D-Asp and L-Asp was significantly different between marine *Crenarchaeota* Group I and *Bacteria* (Mann–Whitney, $P < 0.001$; $n = 60$ for D-Asp and $n = 59$ for L-Asp). Also, significant differences were found in the fraction of cells taking up D-Asp and L-Asp between the different water masses (Kruskal–Wallis, $P < 0.05$; $n = 60$ for D-Asp and $n = 59$ for L-Asp). The percentage of *Bacteria* taking up L-Asp was significantly higher than D-Asp uptake in all the water masses [Mann–Whitney, $P < 0.02$, $n = 9$ for the subsurface; $P < 0.0001$, $n = 19$ for the oxygen minimum, $P < 0.02$, $n = 9$ for the intermediate waters (MSOW and AAIW), $P < 0.001$, $n = 19$ for the deep waters (NEADW and LDW)]. However, the percentage of marine *Crenarchaeota* Group I taking up L-Asp was not significantly different from that taking up D-Asp [Mann–Whitney, $P > 0.5$, $n = 18$ for the oxygen minimum, $n = 9$ for the intermediate waters (MSOW and AAIW), $n = 19$ for the deep waters (NEADW

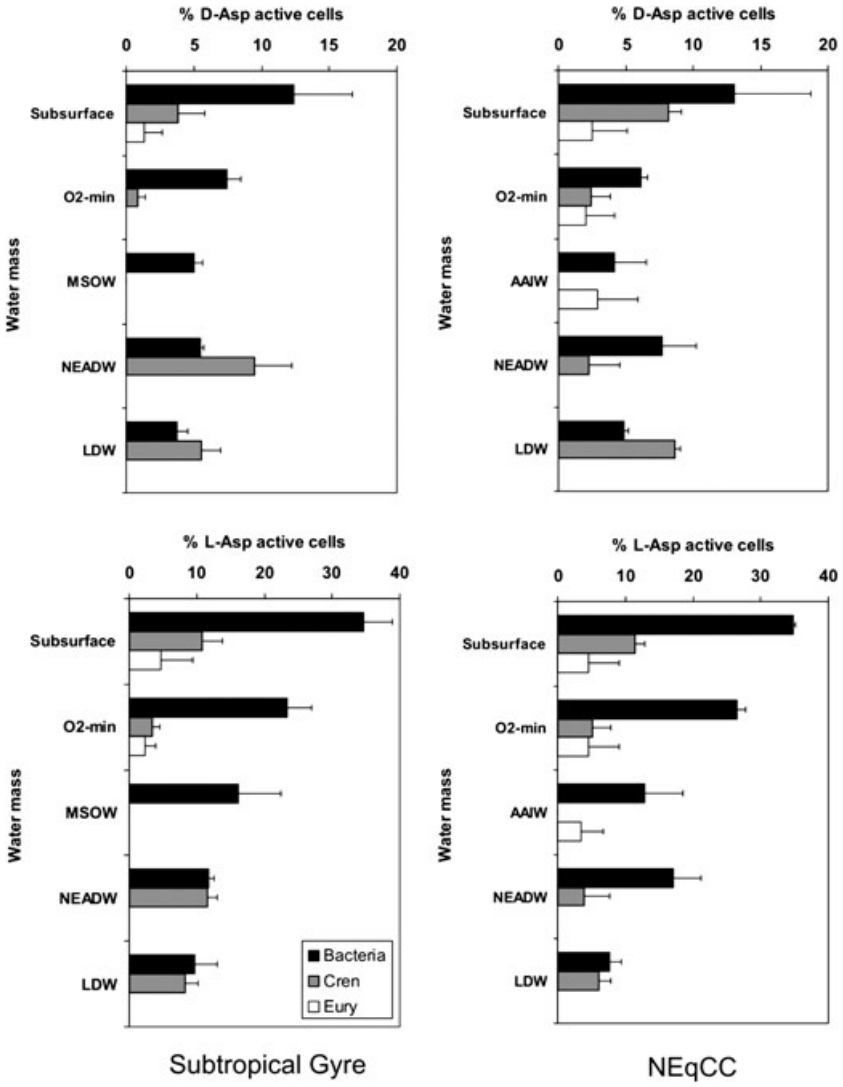

Fig. 4. Percentage of *Bacteria*, marine *Crenarchaeota* Group I and marine *Euryarchaeota* Group II taking up D-Asp and L-Asp in the different water masses. For the Subtropical Gyre, data from Sts. 2, 30 and 36 are given and for the North Equatorial Counter Current (NEqCC), data obtained at Sts. 11 and 23. Bars represent means ± SE. Note the different scale on *x*-axes for percentage D- and L-Asp active cells.

and LDW)] except in subsurface waters, where marine *Crenarchaeota* Group I taking up L-Asp prevailed over those taking up D-Asp (Mann–Whitney, $P < 0.02$, $n = 9$).

Variability in single-cell D- and L-Asp uptake in the different water masses

The average silver grain area of the cells obtained by microautoradiography was linearly correlated with the D- and L-Asp bulk incorporation in the different water masses (Fig. 5). Thus, the silver grain area per cell was used to calculate cell-specific uptake rates of the prokaryotic community. The cell-specific uptake, taking only substrate-positive cells into account, ranged from 0.05 to 0.50 amol D-Asp cell^{-1} day^{-1} and 0.10–2.00 amol L-Asp cell^{-1} day^{-1} among the different water masses. The ratio of cell-specific D-:L-Asp uptake rates increased from the subsurface layer (cell-specific D-:L-Asp uptake ratio ~0.3) to the deeper layers reaching a ratio > 1 in the LDW (St. 2 in the subtropical gyre and St. 23 in the NEqCC) and in the NEADW at St. 36 in the subtropical gyre (Fig. 6, Table 3).

Cell-specific D-Asp and L-Asp uptake rates were higher at the subtropical gyre stations than in the NEqCC (*t*-test, $P < 0.0001$, $n = 1476$ for D-Asp and $P < 0.0001$, $n = 1967$ for L-Asp). In the subtropical gyre, cell-specific D-Asp was higher in the subsurface layer and the upper oxygen minimum layer than in the lower oxygen minimum layer, MSOW and LDW, while no significant difference was found between the subsurface and the NEADW (Fig. 6). Cell-specific L-Asp uptake rates in the subtropical gyre decreased from the subsurface waters towards the deeper water masses (Table 3).

In the NEqCC, cell-specific D-Asp uptake fluctuated only over a rather narrow range from the oxygen minimum layer to the LDW (Table 3). Also, cell-specific L-Asp uptake rates in the NEqCC were higher in the subsurface than in the

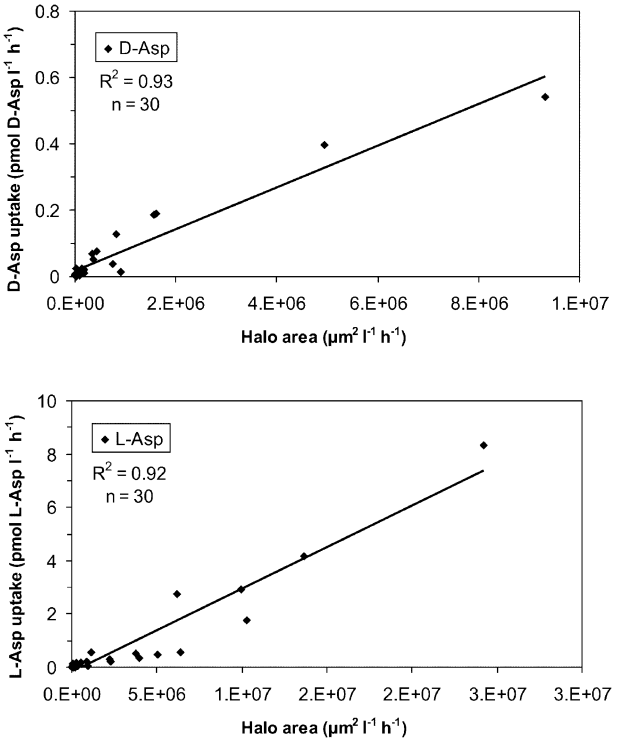

Fig. 5. Relationship between the total silver grain area and bulk D-:L-Asp uptake by the picoplankton community in the different water masses. Data were obtained from Sts. 2, 11, 23, 30 and 36.

oxygen minimum layer, AAIW, NEADW and LDW (Table 3). In the oxygen minimum layer and AAIW, cell-specific L-Asp uptake rates were significantly higher than in the deep-water masses (NEADW and LDW) (Table 3).

Generally, cell-specific D-Asp uptake rates varied within a more narrow range of the activity spectrum than cell-specific L-Asp uptake rates; however, both cell-specific D-Asp and L-Asp uptake rates were skewed towards the lower activity spectrum (Fig. 7). For instance, in the AAIW of the NEqCC, ~50% of the cells exhibited cell-specific D-Asp uptake rates ranging from 0.01 to 0.07 amol D-Asp cell^{-1} day^{-1} while less than 5% of the cells showed activities > 0.40 amol D-Asp cell^{-1} day^{-1} (Fig. 7). In contrast, ~30% of the cells showed cell-specific L-Asp uptake rates in the lower activity classes (between 0.01 and 0.15 amol L-Asp cell^{-1} day^{-1}); however, still ~15% of the cells exhibited activities > 0.60 amol L-Asp cell^{-1} day^{-1}.

Discussion

The North Atlantic Deep Water is formed by several water masses originating in the northern-most parts of the North Atlantic (van Aken, 2000a,b; Rhein *et al.*, 2002), and flows to the south in the eastern basin resulting in the NEADW (Smethie and Fine, 2001). Because of mixing with the underlying Antarctic Bottom Water, the properties of the lower parts of the NEADW gradually change towards the equator. The Antarctic Bottom Water enters the eastern North Atlantic Basin through the Romanche Fracture Zone (at the Mid Atlantic Ridge at 5°S) and flows northwards mixing with the deep NEADW to form the LDW (van Aken, 2000a). Overlying the NEADW, the influence of the MSOW increases the salinity signal (> 36.5) in the subtropical gyre region between 35°N and 15°N (van Aken, 2000b). In the southern part of the transect (from 15°N to 5°N), below the North Equatorial Counter Current, a salinity minimum (< 34.7) is found, representing the AAIW brought into the eastern North Atlantic by the North Brazil Undercurrent (van Aken, 2000b). Apparently, the differences in the origin and history of these deep-water masses do not only lead to distinct salinity-temperature and nutrient characteristics of these water masses clearly identifiable over thousands of kilometres in the global ocean circulation but might also be reflected in the prokaryotic community composition and activity. The prokaryotic community composition and activity of these specific deep-water masses are modified by the upper ocean physical and nutrient conditions and associated to these, the biological productivity and export fluxes. As shown here, differences in the upper ocean characteristics of the NEqCC with its generally higher primary productivity than the suptropical gyre propagate into the deep-water masses.

Prokaryotic distribution in the different water masses

A higher picoplankton abundance was found in the mesopelagic waters (representing AAIW) of the NEqCC than in

Table 3. Average cell-specific uptake rates of D-Asp and L-Asp (amol D- or L-Asp cell^{-1} day^{-1}) in the different water masses of the North Atlantic.

	Subtropical gyre			NEqCC		
Water mass	D-Asp	L-Asp	D:L ratio	D-Asp	L-Asp	D:L ratio
Subsurface	0.32 ± 0.08^{a}	1.26 ± 0.29^{a}	0.27 ± 0.05	0.27 ± 0.03^{a}	0.80 ± 0.07^{a}	0.33 ± 0.01
O_2-minimum	0.22 ± 0.04^{b}	0.74 ± 0.29^{b}	0.40 ± 0.09	0.15 ± 0.02^{b}	0.50 ± 0.09^{b}	0.34 ± 0.07
MSOW or AAIW	0.12 ± 0.02^{c}	0.57 ± 0.23^{b}	0.39 ± 0.20	0.12 ± 0.02^{b}	0.39 ± 0.02^{b}	0.34 ± 0.08
NEADW	0.31 ± 0.09^{ab}	0.64 ± 0.38^{b}	0.83 ± 0.46	0.13 ± 0.05^{b}	0.27 ± 0.002^{bc}	0.48 ± 0.19
LDW	0.12 ± 0.04^{c}	0.24 ± 0.06^{c}	0.47 ± 0.09	0.10 ± 0.02^{c}	0.10 ± 0.03^{c}	1.11 ± 0.55

Subtropical gyre from Sts. 2, 30 and 36 and North Equatorial Counter Current (NEqCC) from Sts. 11 and 23. Mean ± SE is given. Superscript letters indicate significant differences between the different water masses (*t*-test, $P < 0.05$). Water mass abbreviations as in Table 1.

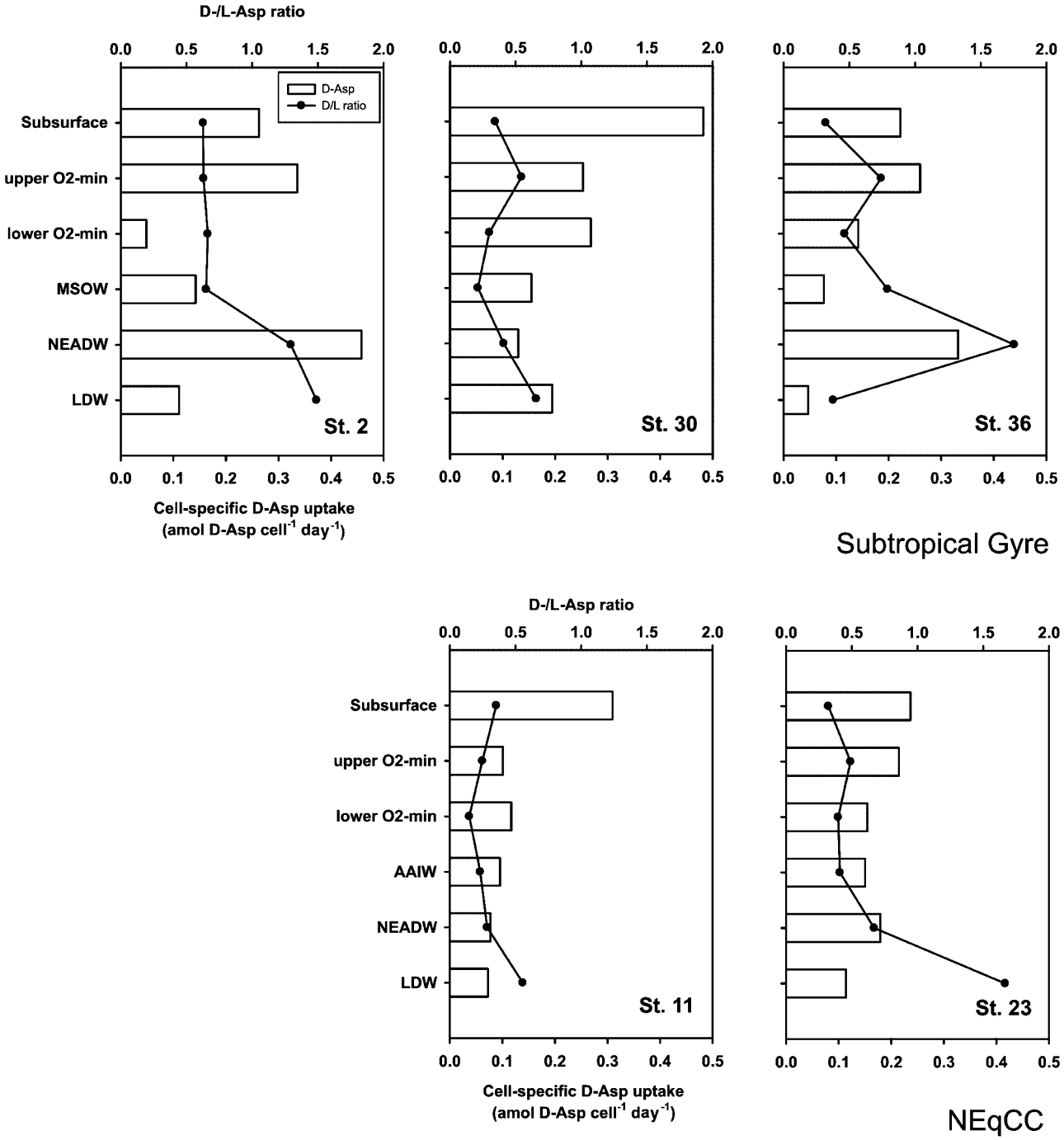

Fig. 6. Average cell-specific D-Asp uptake rates and D-:L-Asp ratio of active prokaryotic cells in the different water masses of the North Atlantic. Subtropical Gyre data are from Sts. 2, 30 and 36 and for the North Equatorial Counter Current (NEqCC) from Sts. 11 and 23.

the subtropical gyre (consisting of MSOW). Also, the bathypelagic waters (NEADW and LDW) sustained a higher picoplankton abundance in the NEqCC than in the subtropical gyre (Table 2). This coincides with the higher inorganic nutrient concentrations (data not shown) of the deep waters in the NEqCC than in the subtropical gyre.

While no differences were found in the mean contribution of *Bacteria* to total picoplankton abundance in the subsurface waters between the subtropical gyre and the NEqCC, the percentage of DAPI-stained cells identified as *Bacteria* in the deep waters of the subtropical gyre was higher than in the deep waters of the NEqCC (Fig. 3). The contribution

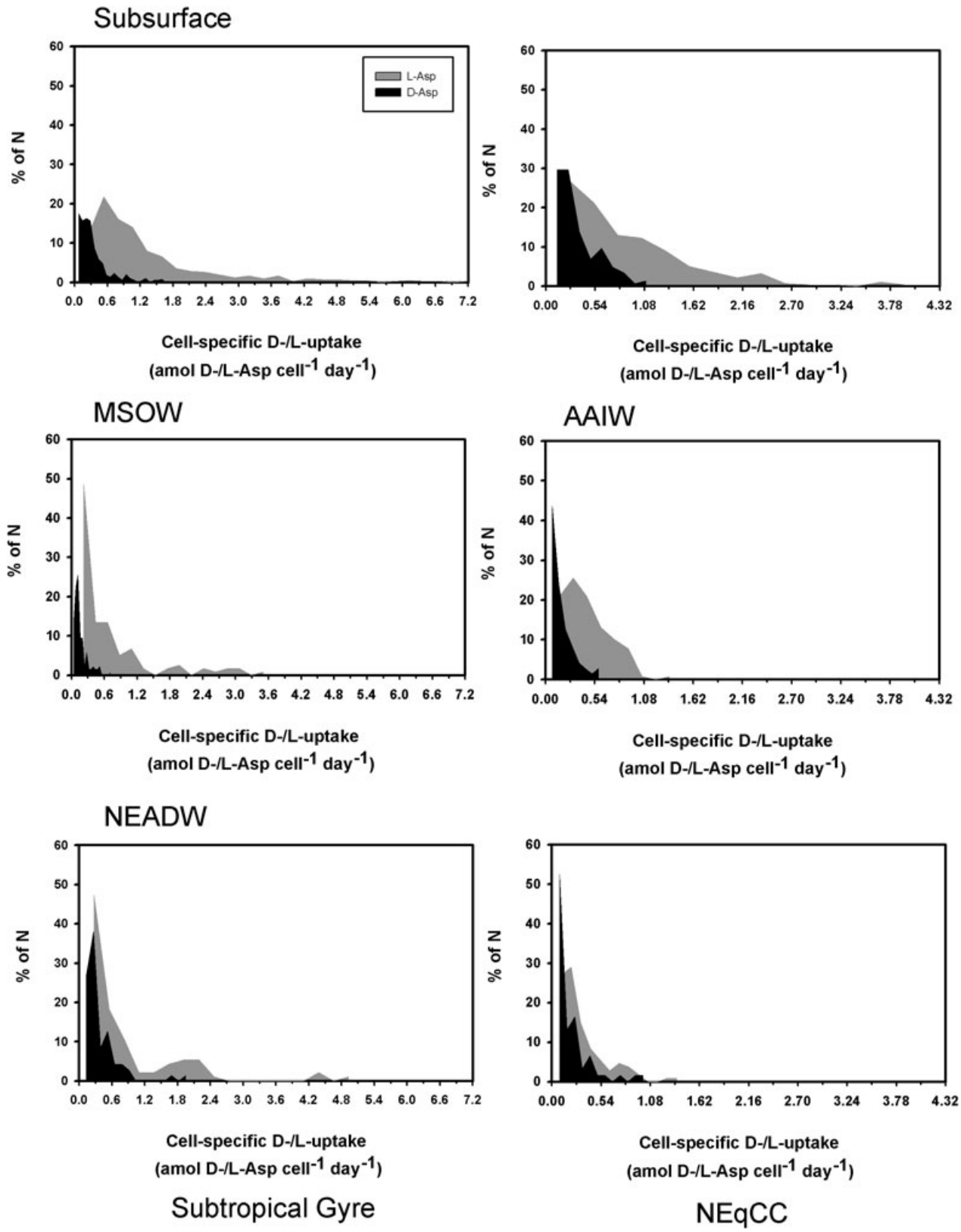

Fig. 7. Distribution of cell-specific D-:L-Asp uptake rates in the subsurface, intermediate (MSOW and AAIW) and deep waters (NEADW) of the North Atlantic. Subtropical Gyre data are from Sts. 2, 30 and 36 and for the North Equatorial Counter Current (NEqCC) from Sts. 11 and 23. The activity classes were determined according to Freedman and Diaconis (1981).

of *Bacteria* to total picoplankton abundance was higher (between 35% and 62%) in the deep-water masses of the subtropical North Atlantic than further north (24–33%) in the North Atlantic (65°N to 35°N) (Teira *et al*., 2006a,b). There is one methodological difference between the studies of Teira and colleagues (2006a,b) and this study as we used the oligonucleotide probe mix Eub338I–III (Daims *et al*., 1999) to enumerate *Bacteria*, whereas Teira and colleagues (2006a,b) used Eub-338 only. It has been shown that the use of Eub-338 is insufficient to detect all *Bacteria* because it does not target members of *Verrucomicrobia* and *Planctomycetales* (Daims *et al*., 1999).

In this study, the recovery efficiency (sum of *Bacteria*, marine *Crenarchaeota* Group I and marine *Euryarchaeota* Group II as a percentage of DAPI-stained cells) ranged between 41% and 66% and was therefore lower than the 66–77% recovery efficiency reported by Teira and colleagues (2006a) using the same CARD-FISH method and oligonucleotide probes for *Crenarchaeota* and *Euryarchaeota*. Our lower recovery efficiency might be caused by the generally lower overall activity of the prokaryotic community in the southern parts of the meso- and bathypelagic waters of the North Atlantic as compared with the northern parts (our unpublished data and Teira *et al*., 2006a). A lower overall prokaryotic activity coincides with a lower rRNA content per cell and hence, potentially resulting in a lower hybridization efficiency. The most likely explanation for our lower recovery efficiency is, however, the presence of a specific prokaryotic group not targeted by one of our oligonucleotide probes. Recently, it has been shown that a deep-branching cluster of *Crenarchaeota* related to a hot spring crenarchaeotal group, pSL12, was abundant below the euphotic zone in the North Pacific Subtropical Gyre which was not detected by the general *Crenarchaeota* probe but only with a cluster-specific probe (Mincer *et al*., 2007). Ongoing cloning and sequencing efforts on the bacterial and archaeal communities of the study site indicate the presence of crenarchaeal sequences in the (sub)tropical North Atlantic not covered by the marine *Crenarchaeota* Group I-specific oligonucleotide probe Cren537 (H. Agogué, unpubl. data). Consequently, we refer in this article exclusively to marine *Crenarchaeota* Group I.

Despite the lower recovery efficiency obtained in this study compared with the studies of Teira and colleagues 2006a,b) further north in the North Atlantic, our results confirm the general distribution pattern of *Crenarchaeota* with depth reported previously (Karner *et al*., 2001; Herndl *et al*., 2005; Teira *et al*., 2006b). The contribution of marine *Crenarchaeota* Group I to total picoplankton abundance is higher in the oxygen minimum layer and bathypelagic waters than in subsurface waters (Fig. 3). We observed a steady increase in the contribution of marine *Crenarchaeota* Group I to the total picoplankton abundance from the subsurface layers down to ~500 m depth. In the present study, the highest contribution of marine *Crenarchaeota* Group I (up to 20% of DAPI-stained cells) was found at Sts. 20 and 22 coinciding with a pronounced oxygen minimum (< 80 μmol kg^{-1}). There is growing evidence that *Crenarchaeota* are particularly associated with low oxygen environments such as in the Black Sea or in upwelling areas (Francis *et al*., 2005; Coolen *et al*., 2007; Lam *et al*., 2007). The oxygen minimum zones are also the main sites of ammonia oxidation (Zehr and Ward, 2002) and recently, the first non-thermophilic *Crenarchaeum* isolated (*N. maritimus*) has been shown to oxidize ammonia (Könneke *et al*., 2005). In the North Atlantic mesopelagic waters, crenarchaeal *amo*A genes are more abundant than betaproteobacterial *amo*A genes, indicating that *Crenarchaeota* might play a significant role in the nitrification process (Wuchter *et al*., 2006). Thus, the high contribution of marine *Crenarchaeota* Group I to total picoplankton abundance detected in the oxygen minimum zone of the North Atlantic might reflect their importance as nitrifiers in these mesopelagic waters (Fig. 3). The oxygen minimum zone was also the depth horizon where the lowest number of crenarchaeal cells taking up Asp was found (Fig. 4), supporting the idea that marine *Crenarchaeota* Group I in this layer are utilizing predominately inorganic carbon as a carbon source and oxidize ammonia as an energy source. At 900 m depth, in both the MSOW and AAIW, a decrease in the crenarchaeal contribution to picoplankton abundance was observed, contributing < 5% to the total picoplankton (Fig. 3). The contribution of marine *Crenarchaeota* Group I increased again (~10% of DAPI stained cells) in the NEADW and LDW, characterized by higher oxygen concentrations than in the overlying water masses, despite being substantially older than the overlying intermediate water masses (Table 1).

Combining the data on the contribution of marine *Crenarchaeota* Group I to total picoplankton abundance of Teira and colleagues (2006a) with those obtained in the present study, latitudinal trends become apparent (Fig. 8). Generally, the contribution of marine *Crenarchaeota* Group I decreases from 65°N towards the equator throughout the water column. While the oxygen minimum zone becomes more pronounced towards the south (oxygen concentration < 50 μmol kg^{-1}, Table 1), the contribution of marine *Crenarchaeota* Group I to total picoplankton abundance as well as the ammonia concentrations declines towards the equator (Fig. 8). The similarity in the distribution pattern between the relative abundance of marine *Crenarchaeota* Group I and ammonia throughout the eastern North Atlantic basin (although not significantly correlated) might indicate that ammonia serves, at least partly, as an energy source for *Crenarchaeota*.

Marine *Euryarchaeota* Group II were found to contribute < 5% to the picoplankton abundance in the deep water

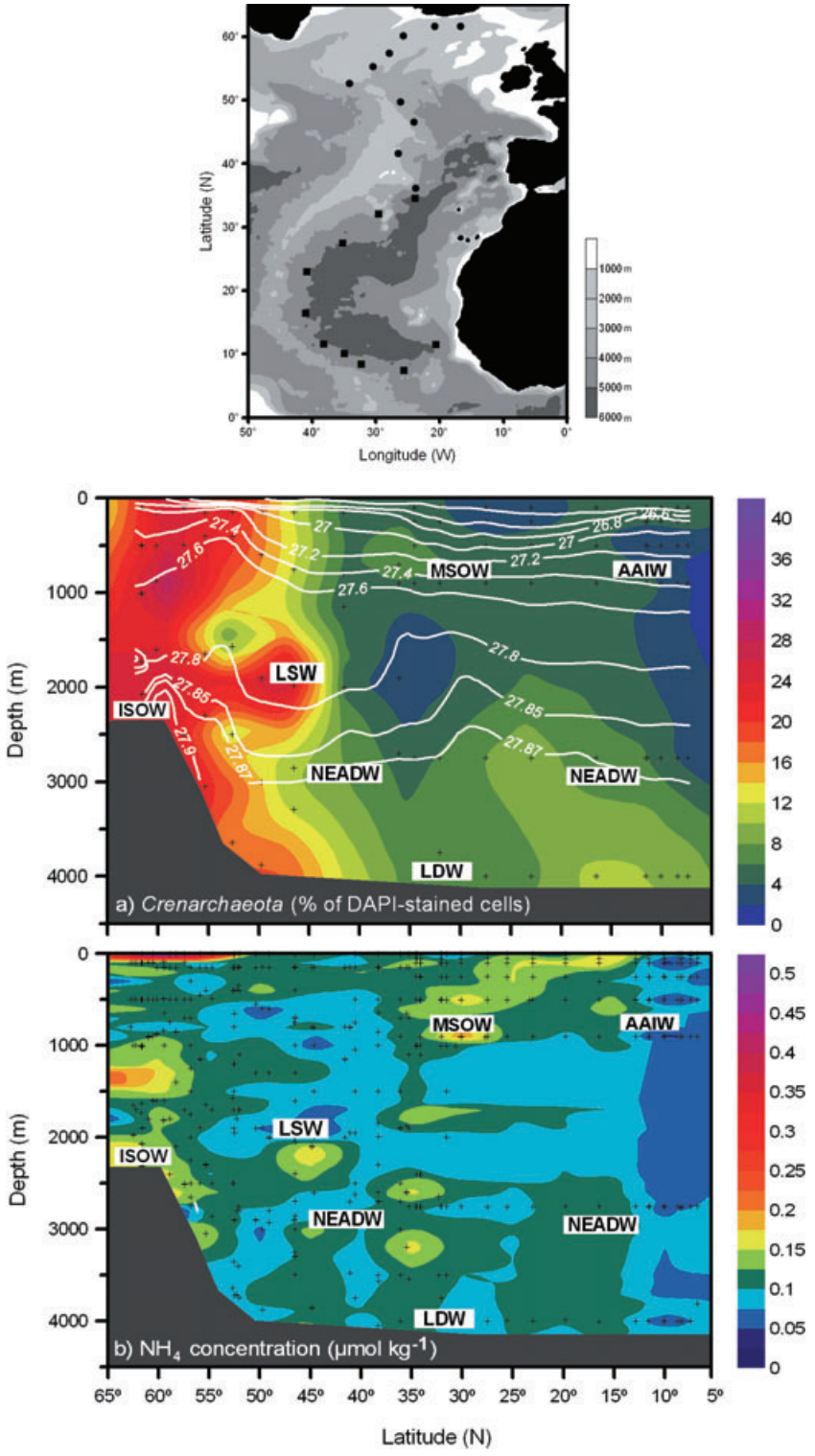

Fig. 8. Contribution of (A) marine *Crenarchaeota* Group I to total picoplankton abundance expressed as percentage of DAPI-stained cells and (B) ammonia concentrations in the eastern basin of the North Atlantic from 65°N to 5°N. In (A), contour lines indicate seawater density in kg m^{-3}. Map of sampling stations (top): squares represent stations occupied during the ARCHIMEDES-I cruise (this article) and circles represent stations occupied during the TRANSAT-I cruise (data from 65°N to 35°N derived from Teira *et al*., 2006a). ISOW, Iceland Scotland Overflow Water, LSW, Labrador Seawater, NEADW, North East Atlantic Deep Water, LDW, Lower Deep Water, MSOW, Mediterranean Sea Outflow Water, AAIW, Antarctic Intermediate Water.

masses below the subtropical gyre waters. Teira and colleagues (2006a,b) reported a higher contribution of marine *Euryarchaeota* Group II, averaging 17% in the Antarctic circumpolar deep waters and 9% in the eastern North Atlantic using the same oligonucleotide probe as used in this study. However, the lower contribution of marine *Euryarchaeota* Group II to the total prokaryotic community reported in this study agrees with studies from similar depth levels in other oceanic basins, reporting a euryarchaeotal contribution < 5–8% of DAPI-stained cells

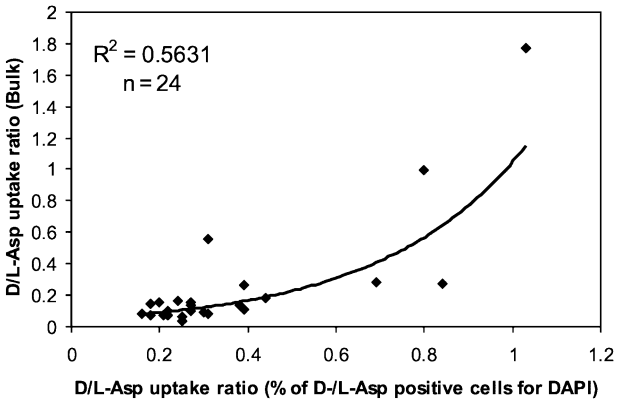

Fig. 9. Relationship between the D-Asp:L-Asp uptake ratio derived from the percentages of active cells obtained by autoradiography and by measuring D-Asp:L-Asp uptake by the bulk prokaryotic community in the different water masses of the North Atlantic.

in the Pacific and in the Antarctic circumpolar deep waters (DeLong *et al*., 1999; Karner *et al*., 2001; Church *et al*., 2003), and in the mesopelagic western Arctic Ocean (Kirchman *et al*., 2007).

Relating prokaryotic community structure and activity measured by D- versus L-Asp uptake in the different water masses of the subtropical North Atlantic

Although it is recognized now that *Archaea* are abundant in the world's ocean (DeLong, 1992; DeLong *et al*., 1994; Karner *et al*., 2001; Teira *et al*., 2006b; Kirchman *et al*., 2007) and recently a non-thermophilic marine crenarchaeote was isolated (Könneke *et al*., 2005), the factors controlling the distribution of the main archaeal groups (*Crenarchaeota* and *Euryarchaeota*) are still largely unknown. While some marine *Crenarchaeota* are putatively oxidizing ammonia, indicated by the presence of the crenarchaeal *amo*A gene (Francis *et al*., 2005; Wuchter *et al*., 2006; Coolen *et al*., 2007; Mincer *et al*., 2007), as an energy source and fix inorganic carbon, hence being autotrophic (Herndl *et al*., 2005; Hallam *et al*., 2006; Ingalls *et al*., 2006; Lam *et al*., 2007), apparently not all marine *Archaea* are autotrophic (Ouverney and Fuhrman, 2000; Herndl *et al*., 2005; Teira *et al*., 2006a).

The obtained D-Asp:L-Asp uptake ratios of the bulk prokaryotic community support previous findings (Pérez *et al*., 2003) that the D-Asp:L-Asp uptake ratio increases with depth (Table 2). Furthermore, the D-Asp:L-Asp uptake ratio derived from the percentages of total active cells obtained by microautoradiography correlates with the D-Asp:L-Asp uptake ratio of the bulk prokaryotic community (Fig. 9). It has also been shown that the increase in the D-Asp:L-Asp uptake ratio from surface to deep waters is largely caused by marine *Crenarchaeota* Group I taking up D-Asp in the deep North Atlantic (Teira *et al*., 2006a). Our data further support the notion that *Crenarchaeota* are efficiently taking up D-Asp in the meso- and bathypelagic waters and extends the geographic region where this pattern is found to the (sub)tropical North Atlantic. While in subsurface waters the percentage of *Bacteria* taking up D-Asp was higher than the corresponding percentage for marine *Crenarchaeota* Group I, in the deep-water masses (NEADW and LDW), marine *Crenarchaeota* Group I exhibited a similar or higher percentage of D-Asp positive cells than *Bacteria* (Fig. 4).

Thus, our results indicate substantial differences in the utilization of enantiomeric amino acids among the major prokaryotic groups. Moreover, the higher D-:L-Asp ratios measured in the northern part of the North Atlantic (Teira *et al*., 2006a) compared with those found in this study might also reflect subtle differences in the dissolved organic matter (DOM) pool of the respective water masses. It has been shown that the chromophoric fraction of DOM increases towards the south corresponding to the increasing ventilation age of these deep waters (Nelson *et al*., 2007). As the NEADW flows southwards and ages, the biological variables also show latitude-related trends.

In this article, we present the first estimates of D- and L-Asp uptake rates on a single-cell level using a quantitative MICRO-CARD-FISH approach (Sintes and Herndl, 2006), taking into account only those cells which are active (Figs 6 and 7). We found that the average cell-specific D-:L-Asp uptake rates are significantly higher in the subtropical gyre (mean 0.22 amol D-Asp and 0.69 amol L-Asp per cell^{-1} day^{-1}) than in the NEqCC (mean 0.15 amol D-Asp and 0.40 amol L-Asp per cell^{-1} day^{-1}) (Table 3). The subsurface waters exhibited higher cell-specific D-:L-Asp uptake rates than meso- and bathypelagic waters, with the exception of the cell-specific D-Asp uptake rates in NEADW of the subtropical gyre, where similar or even higher cell-specific D-Asp uptake rates were found (Sts. 2, 36) than in subsurface waters (Fig. 6). Cell-specific D-Asp uptake rates dominate the lower end of the activity range, while cell-specific L-Asp uptake rates exhibit a broader activity range (Fig. 7). The most remarkable finding is the marked increase of the cell-specific D-:L-Asp uptake ratio with depth. Cell-specific D-:L-Asp uptake ratios were >1 in the NEADW in the subtropical gyre and in the LDW of the NEqCC.

The observations we report here demonstrate that the distribution and activity of the major prokaryotic groups is closely linked to the major water masses of the eastern North Atlantic and not just follow depth-related trends. Our data indicate that in the (sub)tropical North Atlantic (from 35°N to 5°N), *Bacteria* contribute, on average, around 50% to the total picoplankton abundance. Marine *Euryarchaeota* Group II contribute ~5%, while marine *Crenarchaeota* Group I are most abundant in the oxygen minimum layer and in the deep waters (NEADW and

LDW). Single-cell D-:L-Asp uptake rates and ratios indicate an efficient utilization of D-amino acids in the deep waters of the eastern North Atlantic. Finally, by combining data reported previously and data from our study area, a pronounced latitudinal trend in the relative abundance of marine *Crenarchaeota* Group I is apparent, decreasing towards the south and coinciding with decreasing ammonia concentrations. This co-variation between the relative contribution of marine *Crenarchaeota* Group I and ammonia concentrations might indicate that ammonia availability controls to a certain extent the distribution and relative abundance of marine *Crenarchaeota* Group I in the eastern North Atlantic basin.

Experimental procedures

Sampling area

Sampling of meso- and bathypelagic waters was carried out along a more than 9000-km-long transect in the subtropical gyre and the NEqCC of the eastern North Atlantic on board RV *Pelagia* (November/December 2005). For this study, samples were taken at 25 stations out of a total of 42 stations occupied during the ARCHIMEDES-I cruise from six depths: the subsurface (100 m layer); the oxygen minimum layer (average depth 400 m), the MSOW (average depth 900 m) in the subtropical gyre, the AAIW (average depth 900 m) in the NEqCC, the NEADW (average depth 2750 m) and the LDW (average depth 4000 m).

Samples from the distinct water masses were collected with NOEX bottles (no oxygen exchange, 12 l) mounted on a CTD (conductivity, temperature, depth) frame to determine total picoplankton abundance and leucine incorporation, the relative abundance of *Bacteria*, marine *Crenarchaeota* Group I and marine *Euryarchaeota* Group II, the uptake of D-Asp and L-Asp by the bulk picoplankton community and the group-specific D-Asp and L-Asp uptake by MICRO-CARD-FISH as described below.

Picoplankton abundance determined by flow cytometry

Picoplankton collected from the different depth layers of the water column was enumerated using flow cytometry. Samples (2 ml) were fixed with 1% paraformaldehyde (final concentration), shock-frozen in liquid nitrogen for 5 min and stored at – 80°C. Picoplankton cells were stained with SYBR-Green I and enumerated with a FACSCalibur flow cytometer (Becton Dickinson) within 3 months. Immediately before analysis, the thawed picoplankton samples were diluted 5- to 10-fold in TE buffer (10 mM Tris, 1 mM EDTA, pH 8) and stained with SYBR-Green I at room temperature in the dark for 15 min. Fluorescent microspheres (Molecular Probes) with a diameter of 1 μm were added to all samples as an internal standard. Counts were performed with an argon laser at 488 nm wavelength. Picoplankton cells were enumerated according to their right angle scatter and green fluorescence. The counting window of the flow cytometer was set to exclude the occasionally present eukaryotic picoplankton.

Picoplankton production determined by ^{3}H-leucine incorporation

Bulk picoplankton production was measured by incubating 10–40 ml of samples in duplicate and one formaldehyde-killed blank (2% final concentration) with 10 nM [^{3}H]leucine (final concentration, SA 157 Ci mmol^{-1}; Amersham) in the dark at *in situ* temperature for 4 h (Simon and Azam, 1989). Thereafter, the incubation was terminated by adding formaldehyde (2% final concentration) to the duplicate sample. The fixed samples were filtered through 0.2 μm polycarbonate filters (25 mm filter diameter; Millipore) supported by Millipore HAWP filters. Subsequently, the filters were rinsed three times with 10 ml of 5% ice-cold trichloroacetic acid, dried and placed in scintillation vials. Scintillation cocktail (8 ml Canberra-Packard Filter Count) was added and after 18 h, counted in a liquid scintillation counter (LKB Wallac Model 1212). The disintegrations per minute (DPM) of the formaldehyde-fixed blank were subtracted from the mean DPM of the respective samples and the resulting DPM converted into leucine incorporation rates.

Uptake of D-Asp and L-Asp by the bulk prokaryotic community

To measure the uptake of D-Asp and L-Asp by the bulk prokaryotic community, 20–40 ml of duplicate water samples and one formaldehyde-killed blank (2% final concentration) were spiked with either D-[2,3-^{3}H]-Asp or L-[2,3-^{3}H]-Asp (Amersham, SA: D-Asp, 38 Ci mmol^{-1}; L-Asp, 32 Ci mmol^{-1}) at a final concentration of 1 nM and incubated in the dark at *in situ* temperature for 12–48 h. After terminating the incubations by adding formaldehyde (2% final concentration), the samples were filtered through 0.2 μm polycarbonate filters (Millipore, GTTP, 25 mm filter diameter) supported by 0.45 μm cellulose nitrate filters (Millipore, HAWP, 25 mm filter diameter) and rinsed twice with 0.2 μm filtered seawater. The radioactivity was determined as described above for leucine incorporation and the DPM converted to D- and L-Asp uptake rates. A final concentration of radiolabelled Asp (1 nM) was used because the concentration of dissolved free Asp in the deep waters is < 5 nmol l^{-1} and according to Pérez *et al*. (2003), the uptake rates increase from 0.1 to 10 nmol l^{-1} final concentration of added Asp by a factor of 10. Thus, the 1 nM Asp additions represent a compromise between true trace amount addition and obtaining sufficient radiolabel incorporation well above the blank background.

MICRO-CARD-FISH with D-Asp and L-Asp

Water samples of 20–40 ml were spiked with either D-[2,3-^{3}H]-Asp or L-[2,3-^{3}H]-Asp (Amersham, SA: D-Asp, 38 Ci mmol^{-1}; L-Asp, 32 Ci mmol^{-1}) at a final concentration of 1 nM and incubated in the dark at *in situ* temperature for 12–48 h. To the controls, 2% paraformaldehyde (final concentration) was added 15 min prior to radiotracer addition. Incubations were terminated with paraformaldehyde (2% final concentration) and subsequently, the samples stored at 4°C in the dark for 12–18 h. Thereafter, the samples were filtered onto a 0.2 μm polycarbonate filter (Millipore, GTTP, 25 mm filter

diameter) supported by a cellulose nitrate filter (Millipore, HAWP, 0.45 μm), rinsed twice with Milli-Q water, dried and stored in a microfuge vial at – 20°C until further processing in the home laboratory.

Filters for CARD-FISH were embedded in low-gelling-point agarose and incubated either with lysozyme for the *Bacteria* probe mix (Eub338, Eub338II and Eub338III) and for the negative control probe (Non338) or with proteinase-K (for the marine *Euryarchaeota* Group II probe Eury 806 and for the marine *Crenarchaeota* Group I probe Cren537) following the method described by Teira *et al.* (2004). Filters were cut in sections and hybridized with horseradish peroxidase (HRP)-labelled oligonucleotide probes and tyramide-Alexa488 for signal amplification (Teira *et al.*, 2004). Autoradiographic development was conducted by transferring previously hybridized filter sections onto slides coated with photographic emulsion (type NTB-2 melted at 43°C for 1 h). The slides were then placed in a light-tight box containing a drying agent and incubated for exposure at 4°C for 7 days. Finally, the slides were developed and fixed following Kodak's specifications [2 min in Dektol developer (1:1 dilution with Milli-Q water), 10 s in Milli-Q water, 5 min in fixer, and 2 min in Milli-Q water]. Before completely dry, filter sections were removed and cells were counterstained with a DAPI mix [5.5 parts of Citifluor (Citifluor), 1 part of Vectashield (Vector Laboratories) and 0.5 parts of phosphate-buffered saline (PBS) with DAPI (final concentration 5 μg ml^{-1})].

The slides were examined under a Zeiss Axioplan 2 epifluorescence microscope equipped with a 100 W Hg lamp and appropriate filter sets for DAPI and Alexa488. The presence of silver grains surrounding the cells was checked in the transmission mode of the microscope. In the killed controls, < 0.5% of the total DAPI-stained cells were associated with silver grain halos. More than 600 DAPI-stained cells were counted per sample. For each microscope field, four categories were differentiated: (i) total DAPI-stained cells, (ii) cells stained with the specific probe, (iii) DAPI-stained cells with associated silver grain halos and (iv) cells labelled with the specific fluorescent probe and silver grain halos associated with individual cells. Negative control counts (hybridization with HRP-Non338) were always < 1% of DAPI-stained cells.

Image analysis of the silver grain area surrounding active cells

For each sample, two different types of images of the picoplankton cells were acquired: one image for picoplankton stained with DAPI in the epifluorescence mode and one image of the silver grain areas by switching to the transmission mode of the microscope (Sintes and Herndl, 2006). The images were acquired with a digital camera (AxioCam MRc5) mounted on the microscope and overlaid to obtain a composite image. Pictures were taken from 20 to 40 microscopic fields. Per sample, images of 400–800 DAPI-stained cells were recorded. Overlapping signals in the images obtained by DAPI and in the transmission mode of the microscope (silver grain halos) indicated cells taking up the specific enantiomeric amino acid (D- and L-Asp). Image analysis was conducted with the KS300 3.0 software (Carl Zeiss).

The total silver grain area for the whole community was calculated and expressed as the halo area per litre (Sintes and Herndl, 2006). To calculate cell-specific activities, the total silver grain area was then related to the bulk D-Asp and L-Asp uptake of the prokaryotic community following the approach of Sintes and Herndl (2006). Cell-specific activities are given only for the total prokaryotic community as the low number of active marine *Crenarchaeota* Group I and *Euryarchaeota* Group II cells in the individual halo area categories precluded an in-depth analysis.

Statistical analysis

To check normality of the individual data sets, the Kolmogorov–Smirnoff test was used. If normality was not attained, the non-parametric Mann–Whitney (for comparison of two independent variables) and the Kruskal–Wallis (for comparison of three or more variables) test were applied. If data followed normal distribution, the Student's *t*-test was used.

Acknowledgements

We thank the captain and crew of the R/V *Pelagia* for their help during work at sea. Special thanks to E. Teira for making part of the prokaryotic abundance data available shown in Fig. 8 and to A. Smit for performing the enantiomeric aspartic acid uptake measurements at sea. This research was supported by a postdoctoral Fellowship of the Spanish Ministry of Science and Technology (EX2005/0102) and a Marie Curie Fellowship of the European Community (MEIF-CT-2005-023729) to M.M.V. and a grant of the Earth and Life Science Division of the Dutch Science Foundation (ARCHIMEDES project, 835.20.023) to G.J.H. The work was carried out within the frame of the 'Networks of Excellence' MarBef and EurOceans supported by the 6th Framework Program of the European Union.

References

van Aken, H.M., (2000a) The hydrography of the mid-latitude North east Atlantic ocean: I, the deep water masses. *Deep Sea Res Part I* **47:** 757–788.

van Aken, H.M., (2000b) The hydrography of the mid-latitude Northeast Atlantic Ocean: II, the intermediate water masses. *Deep Sea Res Part I* **47:** 789–824.

Church, M.J., DeLong, E.F., Ducklow, H.W., Karner, M.B., Preston, C.M., and Karl, D.M. (2003) Abundance and distribution of planktonic *Archaea* and *Bacteria* in the waters west of the Antarctic Peninsula. *Limnol Oceanogr* **48:** 1893–1902.

Coolen, M.J.L., Abbas, B., Bleijswijk, J.V., Hopmans, E.C., Kuypers, M.M.M., Wakeham, S.G., and Damsté, J.S.S. (2007) Putative ammonia-oxidizing *Crenarchaeota* in suboxic waters of the Black Sea: a basin-wide ecological study using 16S ribosomal and functional genes and membrane lipids. *Environ Microbiol* **9:** 1001–1016.

Daims, H., Brühl, A., Amann, R., Schleifer, K.-H., and Wagner, M. (1999) The domain specific probe EUB338 is insufficient for the detection of all bacteria: development and evaluation of a more comprehensive probe Series System. *Appl Microbiol* **22:** 234–444.

DeLong, E.F. (1992) *Archaea* in coastal marine environments. *Proc Natl Acad Sci USA* **89:** 5685–5689.

DeLong, E.F., Wu, K.Y., Prézelin, B.B., and Jovine, R.V.M. (1994) High abundance of *Archaea*. Antarctic marine picoplankton. *Nature* **371:** 695–697.

DeLong, E.F., Taylor, L.T., Marsh, T.L., and Preston, C.M. (1999) Visualization and enumeration of marine planktonic *Archaea* and bacteria by using polyribonucleotide probes and fluorescent *in situ* hybridization. *Appl Environ Microbiol* **65:** 5554–5563.

Francis, C.A., Roberts, K.J., Beman, J.M., Santoro, A.E., and Oakley, B.B. (2005) Ubiquity and diversity of ammonia-oxidizing archaea in water columns and sediments of the ocean. *Proc Natl Acad Sci USA* **102:** 14683–14688.

Freedman, D., and Diaconis, P. (1981) On this histogram as a density estimator: L2 theory. *Zeit Wahr ver Geb* **57:** 453–476.

Fuhrman, J.A., McCallum, K., and Davis, A.A. (1992) Novel major archaebacterial group from marine plankton. *Nature* **356:** 148–149.

Hallam, S.J., Mincer, T.J., Schleper, C., Preston, C.M., Roberts, K., Richardson, P.M., and DeLong, E.F. (2006) Pathways of carbon assimilation and ammonia oxidation suggested by environmental genomic analyses of marine *Crenarchaeota*. *PLoS Biol* **4:** 520–536.

Herndl, G.J., Reinthaler, T., Teira, E., Aken, H.M.V., Veth, C., Pernthaler, A., and Pernthaler, J. (2005) Contribution of *Archaea* to total prokaryotic production in the deep Atlantic Ocean. *Appl Environ Microbiol* **72:** 2303–2309.

Ingalls, A.E., Shah, S.R., Hansman, R.L., Aluwihare, L.I., Santos, G.M., Druffel, E.R.M., and Pearson, A. (2006) Quantifying archaeal community autotrophy in the mesopelagic ocean using natural radiocarbon. *Proc Natl Acad Sci USA* **103:** 6442–6447.

Karner, M.B., DeLong, E.F., and Karl, D.M. (2001) Archaeal dominance in the mesopelagic zone of the Pacific Ocean. *Nature* **437:** 543–546.

Kirchman, D.L., Elifantz, H., Dittel, A.I., Malmstrom, R.R., and Cottrell, M.T. (2007) Standing stocks and activity of *Archaea* and *Bacteria* in the western Arctic Ocean. *Limnol Oceanogr* **52:** 495–507.

Könneke, M., Bernhard, A.E., de la Torre, J.R., Walker, C.B., Waterbury, J.B., and Stahl, D.A. (2005) Isolation of an autotrophic ammonia-oxidizing marine archaeon. *Nature* **437:** 543–546.

Lam, P., Jensen, M.M., Lavik, G., McGinnis, D.F., Müller, B., Schubert, C.J., *et al.* (2007) Linking crenarchaeal and bacterial nitrification to anammox in the Black Sea. *Proc Natl Acad Sci USA* **104:** 7104–7109.

Mincer, T.J., Church, M.J., Taylor, L.T., Preston, C., Karl, D.M., and DeLong, E.F. (2007) Quantitative distribution of presumptive archaeal and bacterial nitrifiers in Monterey Bay and the North Pacific Subtropical Gyre. *Environ Microbiol* **9:** 1162–1175.

Nelson, N.B., Siegel, D.A., Carlson, C.A., Swan, C., Smethie, W.M., Jr, and Khatiwala, S. (2007) Hydrography of chromophoric dissolved organic matter in the North Atlantic. *Deep Sea Res Part I* **47:** 710–731.

Ouverney, C.C., and Fuhrman, J.A. (2000) Marine planktonic *Archaea* take up amino acids. *Appl Environ Microbiol* **66:** 4829–4833.

Pérez, M.T., Pausz, C., and Herndl, G.J. (2003) Major shift in bacterioplankton utilization of enantiomeric amino acids between surface waters and the ocean's interior. *Limnol Oceanogr* **48:** 755–763.

Rhein, M., Fisher, J., Smethie, W.M., Jr, Smythe-Wright, D., Weiss, R.F., Mertens, C., *et al.* (2002) Labrador Sea Water: pathways, CFC inventory and formation rates. *J Phys Oceanogr* **32:** 648–665.

Simon, M., and Azam, F. (1989) Protein content and protein synthesis rates of planktonic marine bacteria. *Mar Ecol Prog Series* **51:** 201–213.

Sintes, E., and Herndl, G.J. (2006) Quantifying substrate uptake by individual cells of marine bacterioplankton by catalyzed reported deposition fluorescence *in situ* hybridization combined with microautoradiography. *Appl Environ Microbiol* **72:** 7022–7028.

Smethie,W.M., Jr, and Fine, R.A. (2001) Rates of North Atlantic Deep Water formation calculated from chlorofluorocarbon inventories. *Deep Sea Res Part I* **48:** 189–215.

Teira, E., Reinthaler, T., Pernthaler, A., Pernthaler, J., and Herndl, G.J. (2004) Combining catalyzed reported deposition-fluorescence *in situ* hybridization and microautoradiography to detect substrate utilization by *Bacteria* and *Archaea* in the deep ocean. *Appl Environ Microbiol* **70:** 4411–4414.

Teira, E., Aken, H.M.V., Veth, C., and Herndl, G.J. (2006a) Archaeal uptake of enantiomeric amino acids in meso- and bathypelagic waters of the North Atlantic. *Limnol Oceanogr* **51:** 60–69.

Teira, E., Lebaron, P., Aken, H.M.V., Veth, C., and Herndl, G.J. (2006b) Distribution and activity of *Bacteria* and *Archaea* in the deep water masses of the North Atlantic. *Limnol Oceanogr* **51:** 2131–2144.

Wuchter, C., Abbas, B., Coolen, M.J.L., Herfort, L., Bleijswijk, J.V., Timmers, P., *et al.* (2006) Archaeal nitrification in the ocean. *Proc Natl Acad Sci USA* **103:** 12317–12322.

Zehr, J.P., and Ward, B.B. (2002) Nitrogen cycling in the ocean: new perspectives on processes and paradigms. *Appl Environ Microbiol* **68:** 1015–1024.

